Published in Physical Review Letters 35, issue 7, 3062-3068, 1987
which should be used for any reference to this work

Electronic excitations in the transition metals V, Zr, Nb, Mo, and Ta

A. Cornaz,* M. Erbudak, P. Aebi, F. Stucki,† and F. Vanini
Institut für Angewandte Physik, Eidgenössische Technische Hochschule Zürich, CH-8093 Zürich, Switzerland

The np core-loss spectra and the associated deexcitation processes for the transition metals V ($n=3$), Zr, Nb, Mo ($n=4$), and Ta ($n=5$) have been studied in low-energy electron scattering experiments in order to investigate the dependence of their nature on the principle quantum number n. For the metals with $n=3$ and $n=4$, the measurements are accounted for in terms of atomic transitions involving the excitation and the decay of localized d electrons. The observations on V can qualitatively be compared with published computations for isolated atoms. While the $5p$ core excitations for Ta resemble the gross features of the unoccupied d-band density of states, the decay processes involve, besides the conventional O_2VV and O_3VV Auger transitions, autoionization emission related to $5p^65d^N$-$5p^55d^{N+1}$-$5p^65d^{N-1}+\epsilon f$ transitions.

I. INTRODUCTION

A primary electron interacting with an atom can lose energy by exciting a core electron of the target. In the final state there are then two electrons which arbitrarily share the excess energy of the core-level excitation constrained only by the conservation of energy and momentum. One distinguishes two cases. The first one is described by the two electrons well above the Fermi level, E_F, with the atom remaining positively charged. In the case of a $3p$ excitation in a transition metal (TM) with an open $3d$ shell, this state is described by the $3p^53d^N$ configuration. The second limiting case is encountered if one of the electrons is just above E_F, in the vicinity of the neutral atom, which has the configuration of $3p^53d^{N+1}$. In reality, the final state is a superposition of these two possibilities. In the latter case, the atom is excited to a higher level than the first ionization state, and one encounters the case of autoionization. The relaxation of the first possibility occurs via conventional $M_{2,3}VV$ Auger emission and leaves the atom in the doubly ionized $3p^63d^{N-2}$ final state. In the autoionization state there will be interference between p-d direct recombination and d-ϵf emission channels. This autoionization emission leaves the atom in a $3p^63d^{N-1}$ configuration.[1] If these final states differ in energy, the electron-emission spectra will contain both the Auger and autoionization emission at two different kinetic energies.

According to the criterium postulated by Hirst,[2] it is the Coulomb correlation energy U_{eff} between the $3d$ electrons that is responsible for their localization. For such localized states, the energy eigenvalues depend on the occupancy of the $3d$ band. Since the excitation of a $3p$ electron into the $3d$ band, using photons or electrons, is a fast process, not only the adiabatic final states, but also all the possible final states of the excited $3d^{N+1}$ state under the influence of the $3p$ core hole appear in the spectrum. According to Fano,[3] the detailed shape of such an excitation spectrum is determined by the resonant interaction between the different d^{N+1} discrete configurations and the continuum f levels. For the $3d$ TM's, these process have been identified in electron-energy-loss spectroscopy (EELS), in absorption as well as in emission spectra, where autoionization emission appears as an intense high-energy satellite beyond the $M_{2,3}VV$ Auger transitions.[1]

In a model calculation dealing with the $3d$ TM series, Davis and Feldkamp[4] have ascribed the success of the atomic treatment in reproducing the solid-state results to (i) the strong perturbation of the open $3d$ shell caused by the $3p$ core hole, (ii) the narrow $3d$-band width, and (iii) the short time scale for the super-Coster-Kronig transition via which the $3p^53d^{N+1}$configuration decays into $3p^63d^{N-1}\epsilon f$. A more recent phenomenological study has revealed that the energy difference between the observed resonance and the binding energy (E_B) measured with photoemission is large at the beginning of the $3d$ TM series with a less-than-half-full d shell and converges to zero as the d-shell occupation is completed.[1] Bader *et al.*[5] have also observed intense high-energy satellites in EELS beyond the $M_{2,3}VV$ Auger transitions which they ascribe to an autoionization emission.

It is recognized that the excitation and the relaxation processes show (at least for Cr) different angular dependences.[1] Furthermore, the autoionization emission depends on the oxidation state of the atoms, i.e., on the unoccupied density of states (DOS). Therefore, the ϵf-emission intensity is related to the d-band occupancy and shows remnants of bandlike behavior. Recently, Ramsey and Russell[6] observed a transition from atomic to bandlike behavior for Fe, Co, and Ni upon changes in the chemical environment. This complex interplay of atomic and single-particle-DOS effects have also been observed in the $2p$-excitation spectra of the $3d$ TM series.[7]

The purpose of this work is to qualitatively reproduce the EELS results for vanadium using the computed atomic multiplets and to investigate whether the atomic nature of the $3p$-$3d$ excitations prevails for the corresponding $4d$ TM's with broader d bands and even for the $5d$ series where the strong spin-orbit coupling effects on both the

$5p$ and $5d$ wave functions are not negligible. We report on EELS results obtained from single crystals of V, Nb, Mo, Ta, and polycrystalline Zr. Vanadium is chosen as a standard for comparison with earlier results and further along with Nb and Ta in order to investigate the effects of the principal quantum number as one moves to TM's with open $4d$ and $5d$ shells, respectively. Further, we have analyzed both the (100) and (110) surfaces of vanadium in order to find out a possible dependence of the observations on the orientation of the crystalline surface. Zr, Nb, and Mo are at the beginning of the TM series with less-than-half-full $4d$ bands. The $4p$ shells are spin-orbit split by about 2 eV and their binding energies are comparable to those of $3p$ electrons in vanadium. Thus, one would expect the $4p$-hole—$4d$-electron Coulomb interaction to be the strongest mechanism to perturb the $4p$-$4d$ transition process and to lead to atomic excitations. Therefore, they are potential candidates to demonstrate EELS phenomena analogous to those encountered in the $3d$ TM series. Hence, measurements on Zr, Nb, and Mo were performed in order to test the occurrence of the resonances in the $4d$ TM series and to reveal the effects of the d-band occupancy N on the electronic transitions $4p^6 4d^N$-$4p^5 4d^{N+1}$ and the corresponding autoionization emission. For this purpose, electron-energy losses around the p thresholds as well as the emission spectra around the corresponding Auger transitions were recorded. Zr was also measured at 1200 K, above its structural phase transition temperature of 1135 K, in order to test the effects of the crystal structure on the p-d transitions.

The experimental apparatus is described in Sec. II. Section III contains experimental results and outlines the concepts of the Fano formalism in order to compare the results for vanadium with an analytical function derived on the basis of such a theory. The results are discussed in Sec. IV, and conclusions are presented in Sec. V.

II. EXPERIMENTAL

The measurements were performed in an ultrahigh-vacuum (UHV) apparatus with a total pressure in the 10^{-8}-Pa range. Positive ions for sputtering and electrons are produced by means of a hybrid gun.[8] A single-stage cylindrical mirror energy analyzer with a resolution of $\Delta E/E = 0.006$ and a Faraday cage are employed to detect the secondary electrons. The axes of the gun and of the analyzer are aligned perpendicular to each other.[9] V, Nb, Mo, and Ta single-crystal surfaces were oriented with x-ray Laue methods. All samples were polished using diamond powder with gradually decreasing grain size down to 0.3 μm. In UHV, the surfaces were cleaned by repeated cycles of ion etching (2000 eV and 0.1 μA of Ar^+) and heating up to 1000 K until no traces of impurities were detectable by Auger electron spectroscopy. Operating the gun, sweeping the energy analyzer, and data collection were controlled by a preprogrammed personal computer. Secondary-electron spectra were recorded in integral form, in which the electron current was registered by an electrometer, as well as in the second-derivative mode, in which we employed a phase-sensitive detector and modulated the potential at the outer cylinder of the energy analyzer with $2V_{p.p.}$. A second derivative, $d^2N(E)/dE^2$, represents the inverse of the radius of curvature of the function $N(E)$ and hence is extremely sensitive to small changes in the integral form, $N(E)$. Additionally, background is eliminated by this procedure up to a quadratic contribution to $N(E)$. Our experience with EELS has shown that in the negative-second-derivative representation, the energy positions of collective electron oscillations appear as maxima, whereas the thresholds for single-particle excitations are detected as minima. The binding energies of the excited levels lie systematically at slightly higher energies than these minima. This difference is probably due to the different final states in photoemission (excited electron at infinity) and in threshold spectroscopy (excited electron just at E_F).

In all measurements reported here, a primary-electron energy of 350 eV was used. With this energy, the total energy resolution was kept below 2 eV, and it was possible to excite all the energetically possible transitions; at such low excitation energies the momentum transfer of the primary electrons in inelastic collisions is not negligible any more and hence also dipole forbidden transitions occur,[10] such as $3s$-$3d$, which allow us to study the nature of these transitions.

III. RESULTS

A. Vanadium

Figure 1 shows the EELS spectrum obtained from a V(100) surface, both in integral, $N(E)$, and negative second-derivative, $-d^2N/dE^2$, modes.[11] The abscissa represents directly the energy loss in eV with zero as the energy of the elastically scattered electrons. At loss energies of 10.0 and 21.0 eV, two structures are observed representing the plasmon losses.[12] The bulk plasmon-loss

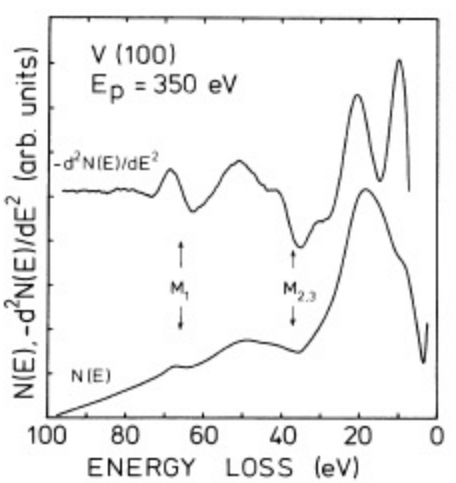

FIG. 1. Electron-energy-loss spectrum (absorption spectrum) obtained from a V(100) surface. The abscissa gives the energy loss in eV. The upper curve is the negative second derivative of the lower one (integral) measured directly applying a modulation voltage of $2V_{p.p.}$ at the energy analyzer.

peak at 21.0 eV shows up 1.0 eV lower in the integral representation; this apparent shift is due to the strong background of secondary electrons that is nearly eliminated in the second derivative. The arrow at 37.1 eV marks E_B of the $3p_{1/2,3/2}$ core levels determined in photoemission experiments.[13] Both spectra show indeed the onset of the $3p$-$3d$ excitation at this energy. However, the transition reaches its maximum (cf. integral curve) at around 50 eV and stretches as far as 60 eV. At 66.0 eV, the dipole-forbidden $3s$-$3d$ transition (M_1) can be observed owing to the low excitation energy of 350 eV,[10] in agreement with $E_B = 66.2$ eV.[13] The general shape of the $3p^6 3d^N$-$3p^5 3d^{N+1}$ excitation spectrum is the same as reported earlier.[1,5] The second derivative, however, resolves some latent structures present in the secondary-electron current, such as at 41.0 eV. A peak at 32.0 eV is detected in the spectrum which can be attributed to a higher-order plasmon loss.

In order to qualitatively analyze EELS data for V, presented in Fig. 1, the contribution of the $3p$-$3d$ transitions has to be isolated from the measured electron current, $N(E)$. In Fig. 2, the raw data for vanadium is shown in the integral representation, $N(E)$ (upper curve), with a cubic spline function[14] simulating the smooth background emission of the inelastically scattered electrons (dotted curve). The curve in the middle is the difference between $N(E)$ and the background, and hence represents the contribution of the $3p$-$3d$ excitations to the measured signal. The vertical bars in the lower part of the figure represent the atomic final-state multiplets of the excited $3p^5 3d^4$ configuration of the vanadium atom, calculated in an intermediate-coupling scheme.[15] Dietz *et al.*[16] have used the Fano formalism in the form of an analytic function $f(E)$ given below, to reproduce the results for Ni, adjusting the line-shape parameter, q, the half-width, Γ, and the position of the discrete level, E^0:

$$f(E) = \sum_i M_i^2 (q_i^2 - 1 + 2q_i\varepsilon_i)(1+\varepsilon_i)^{-2} \qquad (1)$$

with $\varepsilon_i = (E - E_i^0)/\Gamma_i$.

Figure 2 shows (lower curve) $f(E)$ for vanadium where the summation is made over the 8 significant final-state multiplets. For M_i^2 the calculated intensities were used, but the same values of q and Γ for all multiplet components: $q = 0.9$ and $\Gamma = 6$. Nevertheless, the agreement between the calculated results using the atomic data[15] and the experimental curve is relatively good.[11] The spline function that represents the background emission was chosen in such a way that the difference between $N(E)$ and this arbitrary fit qualitatively reproduces the calculated results. To achieve a better agreement, the intensities of the low-energy multiplets should be adjusted. A comparison on the same basis with such adjustments has recently been published;[17] however, the q and Γ values used are slightly different from those stated above. Both observations can be taken as an indication that the discrete final state multiplets interact with the continuum and that the $3p$-$3d$ excitations are of atomic character.

Figure 3 shows the spectrum of secondary electrons for vanadium in the region of the $M_{2,3}VV$ Auger transitions

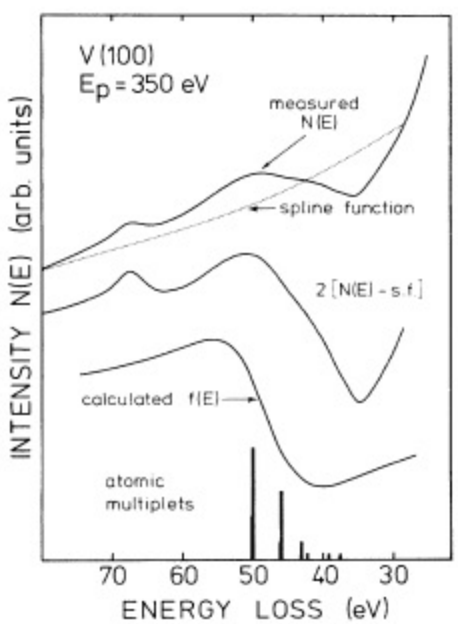

FIG. 2. Electron energy losses in V(100). The upper curve is the raw data, integral electron current, as in Fig. 1, with a spline function (s.f.) (dotted curve) representing the background due to the inelastically scattered electrons. The difference between these two curves is the contribution of the $3p$-$3d$ transitions to the measured spectra and is shown in the middle in twofold amplification. The vertical bars represent the calculated multiplets (Ref. 15). The lower curve results from processing the multiplets using the formalism of Fano resonances (Ref. 3) with $q = 0.9$ and $\Gamma = 6$.

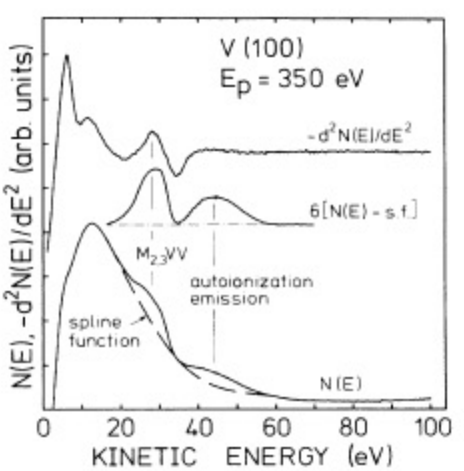

FIG. 3. The electron-emission spectrum from V(100) as a function of electron kinetic energy in eV. Lower curve is the integral representation with a spline background (dashed curve). The sixfold amplified difference curve is in the middle. Upper curve is the negative second derivative of the measured signal. It is used to better identify the latent structures in the integral curve and to determine the energy positions.

as a function of their kinetic energy (a correction in the abscissa for the work function of the collector would shift all energies by 4.0 eV to higher values), both in the integral, $N(E)$ (lower), and the negative-second-derivative (upper) representation. The curve in the middle is the integral curve after subtraction of a cubic spine function in order to eliminate the background. At 28.0 eV the conventional $M_{2,3}VV$ Auger emission is clearly identified in all three curves. The autoionization emission appears with its maximum intensity at 44.5 eV and nearly stretches over an energy region of 20 eV. We have not made any effort to analyze the exact shape of this emission spectrum as the different matrix elements for the Coulomb interaction and the Slater integrals coupling the excited state multiplets with the different continuum states are unknown.

In a similar way, we also investigated a V(110) surface.[11] The excitation and emission spectra obtained were identical with those illustrated above for V(100). Therefore, an effect of the orientation of the surface on the observations can be excluded.

B. Zirconium, niobium, and molybdenum

Figure 4 shows the loss spectra for Zr, Nb(100), and Mo(100) surfaces in the negative-second-derivative representation. All three curves are shifted in energy such that the $4p_{3/2}$ binding energies,[13] N_3, mark the zero of the abscissa. All loss spectra contain three pronounced structures in the energy region well above 20 eV of the $4p$-$4d$ transition thresholds. There are small differences in the positions and the relative intensities of the three curves displayed in the figure. In analogy to the results obtained from vanadium, these structures may represent the final-state $4d$ multiplets broadened by interference effects. As the relevant atomic data for Zr, Nb, and Mo are not available, a quantitative reproduction of these loss spectra was not attempted. It will probably be difficult to treat the excitation processes in the $3d$ and $4d$ TM's on a similar basis owing to the different natures of the d bands involved. Also marked in Fig. 4 are the $4p_{1/2}$ thresholds, N_2. The $3s$ thresholds, N_1, shift, as expected, to higher energies as one goes from Zr to Mo.

The observed structures and their energy spread manifest the atomic behavior of the $4p$-$4d$ excitations. Except for the position of the first peak in the data, which appears at 1.5 eV above each $4p_{3/2}$ threshold, it is impossible to recognize a systematic trend in the spectra obtained from these three TM's without performing a detailed theoretical analysis.

The electron emission spectra for Zr, Nb, and Mo look very similar to that obtained from vanadium. The $N_{2,3}VV$ Auger transitions occur at 21.1, 24.3, and 27.0 eV, respectively, accompanied by a broad autoionization emission contribution centered at 31.2, 35.9, and 38.0 eV.

To investigate a possible influence of the crystal structure on the reported transitions, the measurements on Zr were repeated at 1200 K, well above the structural transformation. As observed in Fig. 5, the excitation spectra for the α and β phases of Zr look very similar. At a kinetic energy of 267 eV (350–83 eV) the carbon KVV Auger signal is detected at elevated temperatures. Indeed the diffusion of carbon and oxygen is drastically enhanced at high temperatures, and it was impossible to obtain a spectrum from an atomically clean surface. Hence, the minor differences in the two spectra in the energy region of the $4p$-$4d$ transitions probably stem from the surface composition of the β phase. Nevertheless, the crystal structure does not affect at least the nature of the p-d transitions.

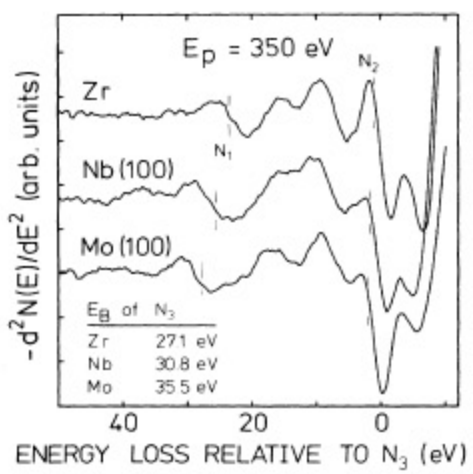

FIG. 4. Energy-loss spectra obtained from $4d$ transition metals Zr, Nb, and Mo. All three curves are shifted in energy such that the $4p_{3/2}$- binding energies (Ref. 13) (N_3) for Zr (27.1 eV), Nb (30.8 eV), and Mo (35.5 eV) coincide and mark the energy zero. The negative second derivatives are shown in order to stress the structures between 0 and 20 eV. Also shown are the binding energies for the $4p_{1/2}$ and $4s$ levels (N_2 and N_1).

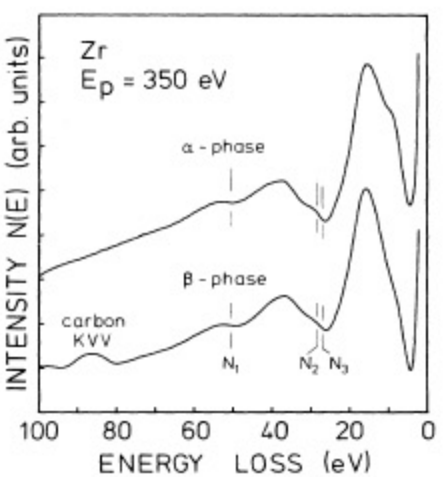

FIG. 5. Energy-loss spectra obtained from α- and β-Zr, measured at 300 and 1200 K, respectively. β-Zr is formed above 1135 K. Note the carbon Auger emission in β-Zr signaling surface diffusion of carbon at elevated temperatures.

C. Tantalum

Figure 6 shows the loss spectrum obtained from a (100) surface of Ta, in the integral, $N(E)$, and negative second derivative, $-d^2N(E)/dE^2$, representations. The curve in the middle is the sixfold multiplication of $N(E)$, after subtraction of a cubic spline function. The surface and bulk plasmons are detected at 7.9 and 19.9 eV, respectively. At 23.6 eV the second derivative shows a dip which can be attributed to the $4f_{5/2}$ excitation (N_6) in accordance with its E_B given by Nyholm *et al.*[18] Thus $4f_{7/2}$-$5d$ transition, N_7, is hidden probably in the huge plasmon signal. The minima at 31.2 and 42.2 eV are assigned to excitations of electrons in the spin-orbit split $5p$-levels[18] (O_3 and O_2). Further in energy, the spectrum shows the $5s$ transition centered at 71.5 eV (O_1).

Figure 7 displays the emission spectrum from Ta(100) in the integral representation, $N(E)$, and its tenfold amplification, after subtraction of the background in form of a spline function. Here, three main structures are identified at 25.2, 34.5, and 44.3 eV. Owing to the large spin-orbit splitting of about 10 eV in the $5p$ levels,[18] the conventional Auger emission shows a doublet shape, each component for a possible hole in the initial state. The two structures at 25.2 and 34.5 eV in the emission spectrum can therefore be assigned to the O_3VV and O_2VV Auger transitions. It is conceivable that the $5d$ electrons of Ta still show some atomlike character in the excited state and interact with the potential of the $5p$ holes. Then one would expect that the interference between the p-d and d-ϵf levels would lead to an autoionization emission. The energy difference of the two resonances thus produced will reflect the splitting of the $5p$ levels. One would further expect that the autoionizing emission is energetically separated from the Auger emission roughly by the half-

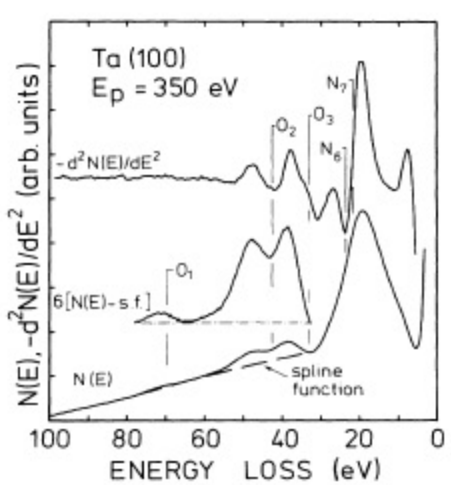

FIG. 6. The secondary-electron current and its negative second derivative obtained from Ta(100) with a primary-electron energy of 350 eV. The measured secondary-electron current, after subtraction of a cubic spline function, gives the curve in the middle, after a sixfold multiplication. The binding energies of various core levels are designated as vertical lines.

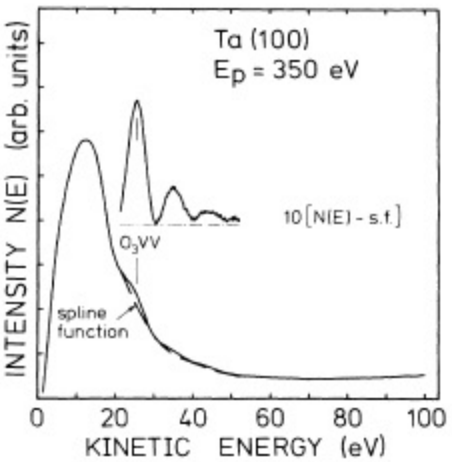

FIG. 7. The spectrum of secondary electrons emitted from Ta(100) in the energy region of the $O_{2,3}VV$ Auger transitions. The integral current and its tenfold amplification after subtraction of a spline background are shown.

width of the occupied $5d$ band plus the energy difference between the observed excitation and E_B. This energy difference is about 10 eV. Generally, in such a case two sets of two emission bands would appear. For Ta, however, the O_2VV Auger line coincides with the autoionization emission via the O_3 hole, at around 35 eV. Therefore, we interpret the structure at around 44.3 eV as belonging to the autoionization emission related to the O_2 hole. The small intensity of this peak indicates that the atomic character of the $5p$-$5d$ transition is not dominant as in the $3d$ and $4d$ TM's displayed above, but it still prevails.

IV. DISCUSSION

The $3p^63d^3$-$3p^53d^4$ excitations in vanadium set in at a threshold very close to the binding energy E_B of the $3p$ levels determined in photoemission experiments. Still, the observed excitation spectrum with an energy spread of nearly 20 eV cannot be reconciled with the unoccupied $3d$-DOS (density of states). This phenomenon has been observed in rare-earth metals for the $4d$-$4f$ transitions and has been accounted for in terms of an atomic model.[19] The success of such a treatment resides mainly in the fact that the $4f$ wave functions are trapped in a centrifugal barrier of the form $l(l+1)r^{-2}$ and behave like electrons in isolated atoms. A fast experiment then shows all the final-state multiplets of the excited $4f^{N+1}$ configuration. In the case of vanadium, the $3d$ band is quite narrow in the ground state and an additional electron acts as a strong perturbation. The overlap of the $3p$ and the $3d$ wave functions favors a strong exchange interaction between the $3p$ hole and the excited $3d$ electrons, which is responsible for the splitting of the $3d^{N+1}$ state in its final-state multiplets. For a d-level occupancy of four, and a singly ionized p level, there are 16×3 possible multiplets.[20] The main lines for the $3p$-$3d$ excitation have been calculated for the vanadium atom[15] in an intermediate-coupling scheme. Fano[3] has shown that a mixing with one or several possible continua influences

the energies as well as the intensities in an asymmetric fashion. Since the published energies and intensities do not include modifications due to such a mixing, corresponding calculations have been performed. The result satisfactorily reproduces the measurements. Incidentally, the mixing with different continua is also responsible for the fact that the relaxation via an autoionization emission and an Auger transition do not occur independently.[21]

A comparison of the $4p$-$4d$ transitions in Zr, Nb, and Mo indicates that the excitation process in these three elements is almost identical,[11] and it is not possible to put forward a systematic dependence between the observed excitation spectra and the $4d$-band occupancy. Also, the emission spectra show only common features, as seen in Fig. 4. It follows that an interpretation of the observations in terms of an atomic picture seems to apply to the $4d$ TM's, too.

The excitation spectra for V, Nb, and Ta are displayed in Fig. 8. The abscissa for each metal is shifted such that the $3p$, $4p_{3/2}$, and $5p_{3/2}$ thresholds coincide with the energy zero. An analysis of the influence of the principal quantum number, i.e., $3p$-$3d$, $4p$-$4d$, and $5p$-$5d$ excitations in the $3d$, $4d$, and $5d$ TM's, cannot be performed self-consistently for several reasons. Whereas, the $3d$ and, to a certain extent, the $4d$ bands are spatially localized, the $5d$ wave functions show an extended nature.[22] The crystal-field and spin-orbit effects are strongest for the $5d$ bands.[23] The $3p$, $4p$, and $5p$ core levels also show differences mainly because of the increasing spin-orbit coupling as one goes from V to Ta. Further, the spatial overlap between the $3p$ and the $3d$ wave functions are almost perfect, while this is not true in Ta for the $5p$ and $5d$ states.

Additionally, for Ta the final-state multiplets have to be calculated in a j-j coupling scheme. We find, however, that the line shapes of the $5p_{1/2}$-$5d$ and $5p_{3/2}$-$5d$ excitations can roughly be reconciled by the unoccupied $5d$-band DOS. A comparison of the empty DOS measured in bremsstrahlung isochromat spectroscopy[24] and the EELS results reported here shows a good agreement.[11] The observable differences between the results obtained in these two spectroscopic methods stem from the core hole present in EELS, which interacts with the excited $5d$ band. The ratio between the intensities of the $5p_{1/2}$ and the $5p_{3/2}$ emission should reflect the same statistical weight as their ground-state occupancies of 1:2. The excitations spectrum from Ta shows a deviation from this ratio. An analogous observation has been made for the $2p$-$3d$ excitations in the $3d$ TM's.[7,25] In that case the intensities of the $2p_{1/2}$ and $2p_{3/2}$ components have been analyzed, which show a spin-orbit splitting comparable to that of the $5p$ electrons in Ta. This observation was interpreted as a deviation of the excitations from a bandlike behavior. The main difference between the $2p$ and $3p$ excitations stems from the nature of these core states and their interaction with the excited $3d^{N+1}$ configuration. The spin-orbit splitting in the $2p$ levels is about 10 eV,[13] whereas it lies within 1 eV for $3p$ core states. The radial distribution of the $2p$ wave functions is less extended compared to that of the $3p$ levels which spatially overlap with the $3d$ states.[22] Therefore, a $3p$ core hole Coulomb perturbation is more effective on the $3d$ wave functions than the effects of the ionized $2p$ levels. One expects that the $2p$-$3d$ excitations require a more profound theoretical treatment taking into account atomic Coulomb and exchange, spin-orbit, and solid-state band-structure effects than is required for the $3p$-$3d$ excitations in vanadium.

The excitation of an s electron into a d band has been possible owing to the breakdown of the dipole selection rules at low excitation energies. All the observed thresholds coincide with E_B. Probably, that the interaction of an s hole with the excited d band is so small that the observed line shapes above the s thresholds cannot be identified with an excitation spectrum of the d^{N+1} electrons but can be understood within the framework of the ground-state one-electron DOS.

The neutralization of the np holes via conventional Auger transitions (super-Coster-Kronig in this case) has been observed in all the metals analyzed here. The emission intensities are generally stronger than the autoionization emission and the linewidths correspond roughly to the self-convolution of the occupied part of the DOS. The energy difference between the Auger and the autoionization emission approximately reflects the sum of the excitation energy of the multiplets above the p threshold and half of the width of the occupied part of the d band.

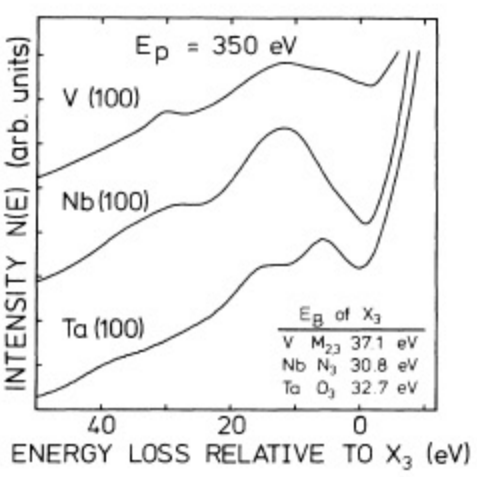

FIG. 8. The excitation spectra for V(100), Nb(100), and Ta(100) in the integral representation. The curves are shifted in energy in order to align the zero energy with the binding energies of $3p_{1/2,3/2}$-, $4p_{3/2}$-, and $5p_{3/2}$-levels, $M_{2/3}$, N_3, and O_3, respectively.

V. CONCLUSIONS

The np core-loss spectra and the related relaxation processes for the TM's V ($n=3$), Zr, Nb, Mo ($n=4$), and Ta ($n=5$) are reported. The $3p$-$3d$ excitations in vanadium metal which have been investigated several times, have been reexamined in this study for comparative purposes. Nevertheless, the observed transition has shown strong features up to 20 eV above the $3p$ threshold, especially in the negative-second-derivative representation of the secondary-electron current, which are interpreted as resulting from the atomic final-state multiplets. Because

the computations for V in this excited state[15] only considered the interaction between the $3d^{N+1}$ state and the ionized $3p$ core level, in this work the different possible channels of relaxation were included within the formalism put forward by Fano.[3] The agreement between the computed and the measured results is very good and manifests the atomic nature of these transitions. Therefore, it is concluded that the exchange energy between the excited $3d^4$ configuration and the $3p$ core hole is at least as large as the width of the d-band DOS in the ground state. Then, the criterium for localization alone, put forward by Hirst,[2] does not suffice to explain the observations, because it is not only the interaction between the different $3d^{N+1}$ electrons which leads to the atomic behavior, but also the interaction of the $3d^{N+1}$ electrons with the potential of the core hole from where the transitions occur. In the case of the $2p$-$3d$ excitations, there still exists the $3d^{N+1}$ configuration, however, because of the lack of $2p$-$3d$ overlap, the core-hole potential is ineffective, and the measured spectra almost reflect the unoccupied part of the $3d$-band DOS.[7]

Since the $4p$-$4d$ excitations observed in Zr, Nb, and Mo resemble those observed in V, the interpretation is extended to the $4d$ TM's. It is concluded that these transitions also reflect atomic behavior.

The excitation spectra are generally influenced by different interactions, e.g., Coulomb, crystal field, spin-orbit, exchange or hybridization. An imbalance of these forces would lead to unexpected observations. For the $3d$ and $4d$ TM's, the Coulomb interaction between the ionized p and d levels dominates. For tantalum, the spin-orbit coupling is predominant, and the total angular momentum j is the good quantum number. Ta shows an ambivalent behavior: the line shapes of the $5p$-$5d$ transitions can be interpreted in terms of a one-electron DOS, whereas the deviation of the O_2- and O_3-emission intensities from the expected statistical weights and the observation of the autoionization emission call for an atomic model.[7,25] The spatial extent, the hybridization with the $6s$ electrons, and the crystal-field interaction of the $5d$ band do not allow at present for an unambiguous description of the $5p$-$5d$ excitations.

A detailed interpretation of these findings must await a quantitative theory of many-body excitations in solids. These data are presented in the hope of offering some guidance in the elaboration of such a theory.

ACKNOWLEDGMENTS

The authors thank G. Kostorz for his continuous support, W. Baltensperger, J. S. Helman, H. C. Siegmann, and E. Tosatti for helpful discussions, and A. Meier for his able technical help. This work was partly supported by the Schweizerische Nationalfonds.

*Present address: Laboratorium für Festkörperphysik, Eidgenössische Technische Hochschule Zürich, CH-8093 Zürich, Switzerland.

†Present address: Brown Boveri Research Center, CH-5405 Baden-Dättwil, Switzerland.

[1]G. Zajac, S. D. Bader, A. J. Arko, and J. Zak, Phys. Rev. B **29**, 5491 (1984).

[2]L. L. Hirst, in *Magnetism and Magnetic Materials—1974 (San Francisco)*, Proceedings of the 20th Annual Conference on Magnetism and Magnetic Materials, AIP Conf. Proc. No. 24, edited by C. D. Graham, Jr., G. H. Lander, and J. J. Rhyne (AIP, New York, 1975), p. 11.

[3]U. Fano, Phys. Rev. **124**, 1866 (1961).

[4]L. C. Davis and L. A. Feldkamp, Solid State Commun. **19**, 413 (1976).

[5]S. D. Bader, G. Zajac, and J. Zak, Phys. Rev. Lett. **50**, 1211 (1983).

[6]M. G. Ramsey and G. J. Russell, Phys. Rev. B **32**, 3654 (1985).

[7]J. Fink, Th. Müller-Heinzerling, B. Scheerer, W. Speier, F. U. Hillebrecht, J. C. Fuggle, J. Zaanen, and G. A. Sawatzky, Phys. Rev. B **32**, 4899 (1985).

[8]E. B. Bas, E. Gisler, and F. Stucki, J. Phys. E **17**, 405 (1984).

[9]U. Bänninger, Ph.D. thesis, Eidgenössische Technische Hochschule, 1974; R. Seiler, Ph.D. thesis, Eidgenössische Technische Hoschschule, 1983.

[10]F. P. Netzer, G. Strasser, and J. A. D. Matthew, Phys. Rev. Lett. **51**, 211 (1983).

[11]A. Cornaz, Diploma thesis, Eidgenössische Technische Hochschule, 1986.

[12]J. H. Weaver, D. W. Lynch, and C. G. Olson, Phys. Rev. B **10**, 501 (1974).

[13]J. C. Fuggle and N. Mårtensson, J. Electron Spectrosc. Relat. Phenom. **21**, 275 (1980).

[14]M. Deutsch and I. Beniaminy, Rev. Sci. Instrum. **53**, 90 (1982).

[15]F. Combet Farnoux and M. Lamoureux, in *Vacuum Untraviolet Radiation Physics,* Proccedings of the Fourth International Conference on Vacuum Ultraviolet Radiation Physics, edited by E.-E. Koch, R. Haensel, and C. Kunz (Pergamon, Hamburg, 1974).

[16]R. E. Dietz, E. G. McRae, Y. Yafet, and C. W. Caldwell, Phys. Rev. Lett. **33**, 1372 (1974).

[17]S. D. Bader, G. Zajac, A. J. Arko, M. B. Brodsky, T. I. Morrison, N. Zaluzec, J. Zak, R. L. Benbow, and Z. Hurych, Phys. Rev. B **33**, 3636 (1986).

[18]R. Nyholm, A. Berndtsson, and N. Mårtensson, J. Phys. C **13**, L1091 (1980).

[19]A. F. Starace, Phys. Rev. B **5**, 1773 (1972); J. Sugar, *ibid.* **5**, 1785 (1972); J. L. Dehmer and A. F. Starace, *ibid.* **5**, 1792 (1972).

[20]J. C. Slater, *Quantum Theory of Atomic Structure* (Prentice-Hall, New York, 1963).

[21]F. Combet Farnoux, Phys. Rev. A **25**, 287 (1982).

[22]F. Herman and S. Skilman, *Atomic Structure Calculations* (Prentice-Hall, New York, 1963).

[23]J. Keller (private communication).

[24]V. Dose, Appl. Phys. **14**, 117 (1977).

[25]J. Zaanen, G. A. Sawatzky, J. Fink, W. Speier, and J. C. Fuggle, Phys. Rev. B **32**, 4905 (1985).